Cell

M. tuberculosis and *M. leprae* Translocate from the Phagolysosome to the Cytosol in Myeloid Cells

Nicole van der Wel,[1,4] David Hava,[2] Diane Houben,[1] Donna Fluitsma,[3] Maaike van Zon,[1] Jason Pierson,[1] Michael Brenner,[2] and Peter J. Peters[1,*]
[1] The Netherlands Cancer Institute, Antoni van Leeuwenhoek Hospital, Plesmanlaan 121, 1066 CX Amsterdam, The Netherlands
[2] Brigham and Women's Hospital and Harvard Medical School, Boston, MA 02115, USA
[3] VU Medical Centre, Department of Molecular Cell Biology and Immunology, Amsterdam, the Netherlands
[4] Present address: VU Medical Centre, Department of Medical Microbiology and Infection Control, Amsterdam, The Netherlands.
*Correspondence: p.peters@nki.nl
DOI 10.1016/j.cell.2007.05.059

SUMMARY

M. tuberculosis and *M. leprae* are considered to be prototypical intracellular pathogens that have evolved strategies to enable growth in the intracellular phagosomes. In contrast, we show that lysosomes rapidly fuse with the virulent *M. tuberculosis*- and *M. leprae*-containing phagosomes of human monocyte-derived dendritic cells and macrophages. After 2 days, *M. tuberculosis* progressively translocates from phagolysosomes into the cytosol in nonapoptotic cells. Cytosolic entry is also observed for *M. leprae* but not for vaccine strains such as *M. bovis* BCG or in heat-killed mycobacteria and is dependent upon secretion of the mycobacterial gene products CFP-10 and ESAT-6. The cytosolic bacterial localization and replication are pathogenic features of virulent mycobacteria, causing significant cell death within a week. This may also reveal a mechanism for MHC-based antigen presentation that is lacking in current vaccine strains.

INTRODUCTION

Initial host-pathogen encounters include bacterial interactions with epithelial tissues that serve as physical barriers to invasion and infection. Additionally, host phagocytes and antigen-presenting cells, such as macrophages and dendritic cells (DCs), have a significant role in innate host resistance to infection and contribute to the generation of adaptive immune responses. These myeloid cells internalize microbes into membrane-bound organelles termed phagosomes that mature and fuse with lysosomes. Phagolysosome fusion creates an acidic environment rich in hydrolytic enzymes that degrade and kill bacteria. Moreover, proteolysis of bacteria in these compartments generates antigens that may elicit MHC- or CD1-restricted T cell responses.

Intracellular pathogens commonly avoid lysosomal fusion through the manipulation of host signal transduction pathways and the alteration of endocytic traffic resulting in privileged replicative niches. In contrast, *Listeria monocytogenes* and *Shigella flexneri* lyse the phagosomal membrane and escape from the endocytic system into the host cytosol, where they replicate and are able to spread to neighboring cells via actin-based motility (Stevens et al., 2006). Nearly all intracellular pathogens have specialized to manage their fates as "endosomal" or "cytosolic" pathogens. Despite the partial cytosolic localization with low percentages of *Mycobacterium marium* (Stamm et al., 2003, 2005), it is currently thought that the most successful pathogenic mycobacterium, *M. tuberculosis*, persists and replicates within the phagosomes of macrophages. Here it prevents lysosomal fusion and maintains extensive communication with early endosomal traffic in a fashion that is thought to provide access to nutrients for survival and growth. (Orme, 2004; Vergne et al., 2004; Russell et al., 2002; Kang et al., 2005; Russell, 2001; Pizarro-Cerda and Cossart, 2006). In this study we arrive at a different conclusion.

RESULTS

M. tuberculosis and *M. leprae* Reside in a Phagolysosome Early after Phagocytosis

The subcellular localization of *M. tuberculosis* and *M. leprae* was analyzed in freshly isolated human monocyte-derived DCs. DCs were differentiated from human CD14+ monocytes precursors for 5 days in GM-CSF and IL-4 and were subsequently infected with *M. tuberculosis* H37Rv or *M. leprae.* Samples were fixed at various times after infection (2–48 hr) and processed for cryo-immunogold electron microscopy (Peters et al., 2006). We analyzed the localization of early and late endosomal markers to the *M. tuberculosis* or *M. leprae* phagosome. Two hours after infection, the phagosome lacked the early

Table 1. Immunogold Labelling of Several Markers Specific for Different Cellular Compartments which Were Present (+) or Absent (–) on *M. tuberculosis*- or *M. leprae*-Containing Phagosomes in DCs Infected for 2 Hr

Compartment	Marker	*M. tuberculosis*	*M. leprae*
ER	PDI	–	–
	MHC I	–	–
	TAP	–	–
Early Endosome	TfR	–	–
	EEA1	–	–
Late Endosome	M6PR	–	–
Lysosome	CD63	+	+
	LAMP-1	+	+
	LAMP-2	+	+
	Cathepsin D	+	+

endosomal markers transferrin receptor (TfR) and early endosomal autoantigen 1 (EEA1), which instead were exclusively localized to early endocytic and recycling endosome membranes (Table 1). The phagosome was also negative for the late endosomal cation-independent mannose 6-phosphate receptor (Table 1). In contrast, both *M. tuberculosis* and *M. leprae* phagosomal membranes labeled for the lysosomal associated membrane proteins LAMP-1, LAMP-2, and CD63 and the major lysosomal aspartic proteinase cathepsin D (Figures 1A–1D; Table 1). In immature DCs, these markers differentially localize in multivesicular and multilamellar lysosomes such as the MHC class II compartment (MIIC; Peters et al., 1991), with LAMP-1 and LAMP-2 localized on the limiting membrane, CD63 on internal membranes, and cathepsin D in the lumen. Following the maturation of DCs, the multivesicular/multilamellar nature of MIICs is modified, and all transmembrane proteins (LAMP-1, LAMP-2, and CD63) localize to the limiting membrane of the mature DC lysosome (MDL; van der Wel et al., 2003). The efficient delivery of these molecules to the phagosome following infection was visualized by the direct fusion of multivesicular lysosomes with the phagosome (Figures 1B and 1B′, arrow heads).

The fusion of lysosomes with the *M. tuberculosis* phagosome at early time points led us to investigate whether LAMP-1 accumulated on phagosomes over time. Over the course between 2 and 48 hr of infection, the average labeling density of LAMP-1 on *M. tuberculosis* and *M. leprae* phagosomes remained stable (Figure 2A) and had levels that were only slightly lower than the lysosomal membranes monitored in the same cells. To determine if the ER contributed to the phagocytosis of either microbe, immunogold labeling was performed on thawed cryosections for MHC class I and two ER resident proteins: the cytosolic epitope of MHC class I peptide transporter (TAP) and protein disulphide isomerase (PDI), a soluble ER protein. None of these molecules was detected within or on *M. tuberculosis* or *M. leprae* phagosomal membranes at multiple time points (Table 1; Figure S1). Quantification of the MHC class I labeling density in the ER and on the phagosomal membrane demonstrated that the levels in the phagosome do not rise above background levels of labeling seen in mitochondria (Figure S1). Furthermore, despite the close proximity of ER cisternae to the phagosomal membrane, fusion between the membranes was not observed ($n > 1000$). Thus, following the infection in DCs, the mycobacteria reside in a compartment that readily fuses with lysosomes and forms independent of the ER.

Live *M. tuberculosis* and *M. leprae* Translocate from the Phagolysosome to the Host Cytosol of Nonapoptotic Cells

It is thought that in macrophages, the access of the phagosome to the early endocytic system enables *M. tuberculosis* and *M. leprae* to evade acidification and degradation and permits growth by allowing extracellular nutrients to reach replicating bacteria. The localization of almost all *M. tuberculosis* to a phagolysosomal compartment in DCs during the first two days of infection led us to investigate acidification of the phagosomes. Lysotracker-Red experiments demonstrated that after 20 hr of infection with live *M. tuberculosis* 24% of the phagosomes were acidified, while 87% of phagosomes infected with dead bacteria were acidified at the same time point. These results suggest that in 76% of *M. tuberculosis* containing phagolysosomes the bacteria are not likely exposed to degradation.

To investigate the intracellular survival and growth in these compartments, DCs were infected with *M. tuberculosis* and plated in replicate wells of a 24-well plate. At each time point, DCs were lysed, and the number of colony-forming units (CFU) per well was enumerated. During the initial 48 hr of infection, the titer of *M. tuberculosis* remained constant, indicating no net growth in DC culture over this time (Figure 2B). Throughout this time period, *M. tuberculosis* were found exclusively in phagolysosomes, as shown above (Figure 1).

The slow-growth kinetics of *M. tuberculosis* and the failure of early endocytic vesicles to reach the phagolysosome during the first 48 hr of infection indicate that the phagolysosomal compartment restricts bacterial replication. However, following this period, the titer of *M. tuberculosis* increased steadily over the next 48 hr of culture (Figure 2B). In later experiments, similar growth kinetics were observed, and the bacterial CFU titer continued to increase between 3 and 7 day postinfection (data not shown). Thus, *M. tuberculosis* persist during the initial 48 hr infection period in DCs but are able to replicate significantly only after that time point. The increase in bacterial CFU titer after day two suggested that alterations occur to the phagolysosome that create a more favorable growth environment. To investigate the intracellular localization of the bacteria in this timeframe, DCs infected with

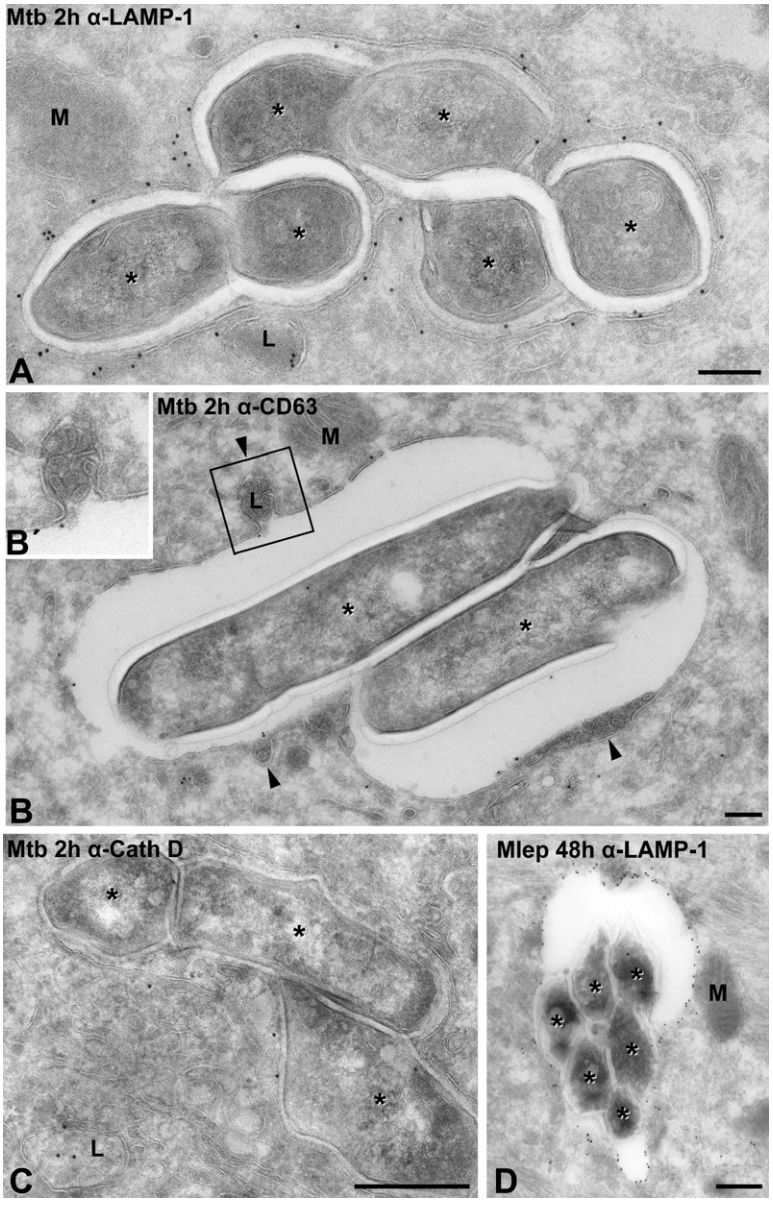

Figure 1. In Early Stages of Infection, *M. tuberculosis* and *M. leprae* Reside in LAMP-1- and Cathepsin-D-Containing Phagolysosomes

(A) LAMP-1 labeling on phagosomal membrane early in infection. Immunogold labeling of LAMP-1 on a DC infected with *M. tuberculosis* for 2 hr on phagolysosomes and lysosomes. For comparison there is no background labeling on the mitochondrium in the same cell. Note that only membranes, perpendicular present in section direction, can be properly stained and thus visualized in cryosections, as these are negatively stained by Uranyl acetate. Therefore, membranes appear as electron-lucent structures surrounded by an electron-dense substrate.

(B) Fusion of lysosomes with CD63 labeled phagosomal membrane. CD63 labeling on the limiting membrane of the phagolysosome in a DC infected with *M. tuberculosis* for 2 hr. In addition to labeling, several fusion events of lysosomes with the phagolysosome are visible (arrowheads). Note the electron-lucent zone between the phagosomal membrane and the electron-lucent bacterial cell wall.

(B′) Enlargement of (B) showing fusion event between the limiting membrane of a (multivesicular) lysosome and the phagolysosomal membrane.

(C) Cathepsin D present in the phagosomes early in infection. DC infected with *M. tuberculosis* for 2 hr and immunogold labeled for cathepsin D. Label is present in lysosomes and in the phagolysosome.

(D) *M. leprae* localized in LAMP-1 labeled phagosome. Labeling of LAMP-1 on phagolysosome of DC infected with *M. leprae* for 48 hr.

Asterisks indicate mycobacteria in phagolysosomes, M indicates mitochondrium, L indicates lysosome, and arrowheads indicate fusion profiles. All images are from cryo-immunogold-labeled cryosections. Error bars are as follows: (A) 250 nm, (B) 200 nm, (C) 400 nm, and (D) 300 nm.

M. tuberculosis were fixed and processed for immunofluorescence (van der Wel et al., 2005) or cryo immunogold labeling with anti-LAMP-1 and anti-cathepsin D antibodies. After 4 hr of infection, *M. tuberculosis* primarily localized to LAMP-1- and cathepsin-D-positive phagolysosomes, and the amount of bacteria that resided in LAMP-1- or cathepsin–D-negative compartments was negligible (Figure 2C). At 48 hr after infection, occasionally, bacteria were found that lacked the characteristic electron lucent zone (Armstrong and Hart, 1971) and did not label for LAMP-1 (Figures 3A, 3A′, and A″). Importantly, these bacteria were not present in membrane-enclosed compartments and were localized to the cytosol. Strikingly, inspection of cells infected for 96 hr revealed that the percentage of cytosolic *M. tuberculosis* increased with a function of time and that larger clusters of bacteria were observed which were not in LAMP-1- or cathepsin-D-positive compartments (Figures 2D and 3B). High-magnification images and movies of electron tomographic reconstructions of individual bacteria confirmed that these bacteria lacked phagolysosomal membranes despite residing in close proximity to LAMP-1- or cathepsin-D-positive lysosomes (Figures 4A–4D and S2). Clusters of *M. tuberculosis* present in the cytosol are abundant in DCs infected for 4 and 7 days. Of all the non-apoptotic infected DCs counted at days four and seven about 32% and 57%, respectively, had cytosolic mycobacteria. From these results, we conclude that at later stages after infection a large subset of intracellular *M. tuberculosis* reside in the cytosol of a large proportion of

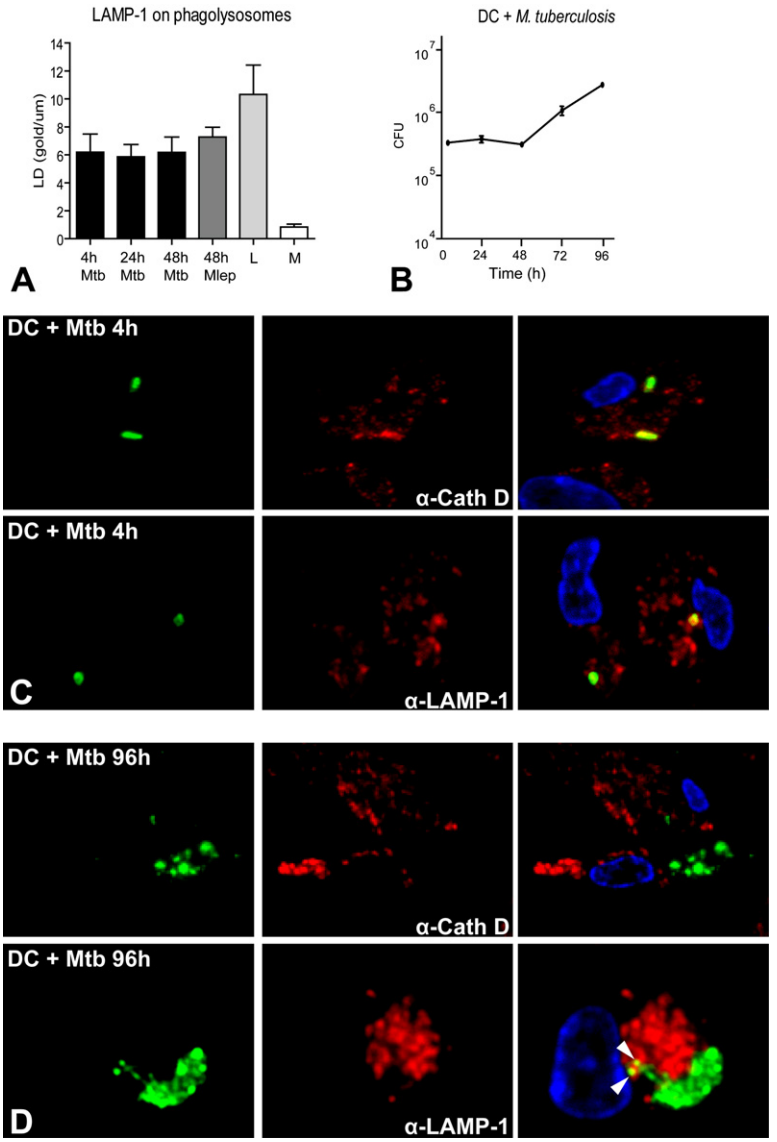

Figure 2. The Relative Amount of *M. tuberculosis* in DCs Increases after 48 Hours of Infection, which Coincides with a Substantial Translocation from the Phagolysosome to the Cytosol

(A) LAMP-1 labeling density on phagosomes and lysosomes. LAMP-1-labeling density (LD): number of gold particles per μm phagosomal membrane as determined on at least 30 phagolysosomes in DCs infected with *M. tuberculosis* for 2, 24, and 48 hr and *M. leprae* for 48 hr remains equal and, compared to the LD on the limiting membrane of lysosomes (L), slightly lower. For comparison the background labeling on the mitochondria (M) in the same cells is negligible. Error bars represent standard error.

(B) Replication *M. tuberculosis* increases after 48 hr of infection in DCs. The colony-forming units (CFU) determined for *M. tuberculosis*-infected DCs. Multiple experiments, from which a representative figure is shown, all demonstrated that the CFU increased after 48 hr, suggesting that replication was significantly (small error bars, representing standard error) initiated after 48 hr of infection.

(C) *M. tuberculosis* colocalizes with LAMP-1 and cathepsin D after 4 hours. Fluorescence image of DCs infected with *M. tuberculosis* (green) for 4 hr labeled with anticathepsin D (red) or LAMP-1 (red) and DAPI (blue) demonstrates that at early stages the bacteria are present in a phagolysosomal compartment. Merged images on the right panel.

(D) No colocalization of *M. tuberculosis* with LAMP-1 and cathepsin D after 96 hours. Fluorescence images of DCs infected for 96 hr in which large clusters of *M. tuberculosis* (green) bacteria are present. Most of these clusters do not colocalize with the lysosomal markers cathepsin D (red) and LAMP-1 (red), although individual bacteria were shown (arrow head) to colocalize. Merged images are on the right panel.

cells. *M. leprae* infected DCs examined at 4 and 7 days after infection (Figures 4E and S2B) were also found in the cytosol.

To determine if the appearance and large clusters of cytosolic bacteria could be associated with growth of *M. tuberculosis*, the number of phagolysosomal bacteria and cytosolic bacteria were quantified over time using the absence of LAMP-1 labeling and a phagolysosomal membrane as obligatory features. The number of cytosolic *M. tuberculosis* per cell rose sharply between 2 and 4 days, increasing approximately 10-fold, while the number of phagolysosomal bacteria increased at a much slower rate (Figure 4F). Likewise, larger clusters of *M. tuberculosis* were observed in the cytosol than in phagolysosomes. This progressively increased over time to an average of 13 bacteria in a cluster per cell in 4 days in the cytosol, while those numbers remained around six in the phagolysosome for the wild-type *M. tuberculosis*. In no instances did we observe LAMP-1 in the absence of phagosomal membrane, confirming our ability to observe membranes surrounding the bacteria. Similar observations were made in *M. tuberculosis*-infected human monocyte-derived macrophages (Figure S3) and THP1 cells (not shown) after 4 days.

To determine if phagolysosomal translocation required an active process of mycobacteria, we examined the localization of heat-killed *M. tuberculosis* in DCs and macrophages. In both cell types, heat-killed *M. tuberculosis* resided exclusively in phagolysosomes that were positive for LAMP-1 (Figure 4G). It is noteworthy that the number of heat-killed bacteria per phagolysosome is comparable to the number of phagosomal bacteria in the live infection, indicating that bacterial burden alone in the phagolysosome is not sufficient for the cytosolic phenotype.

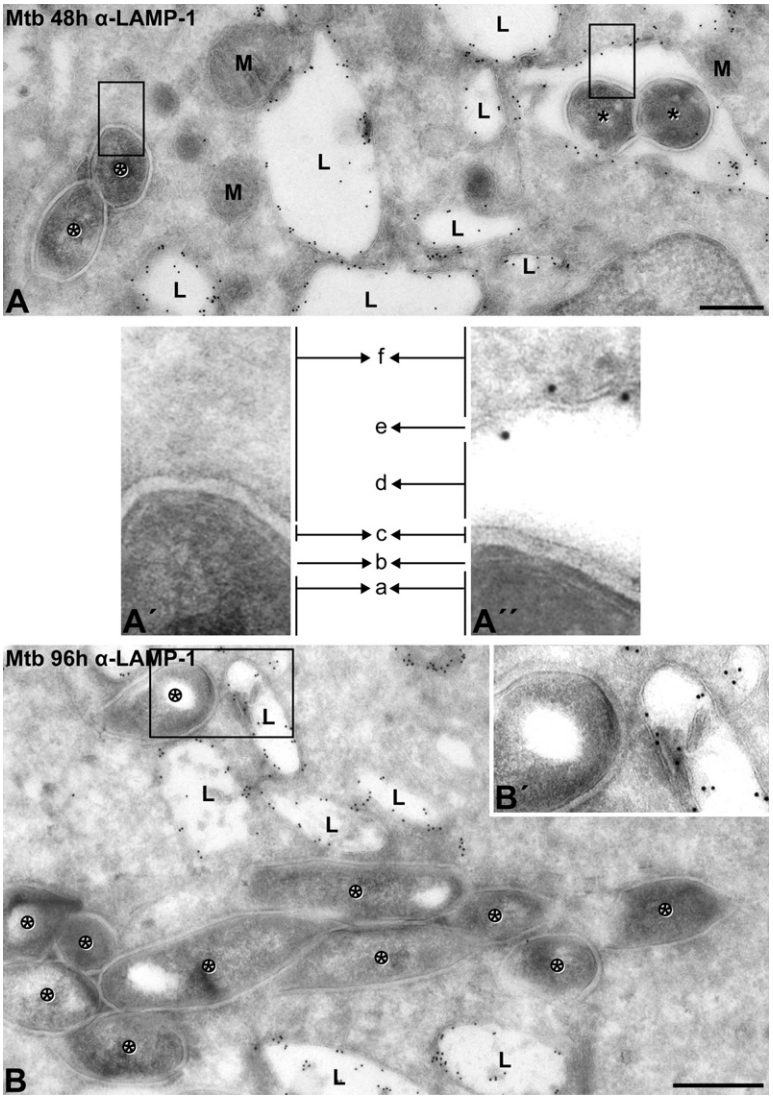

Figure 3. Translocation from the Phagolysosome to the Cytosol at High Resolution

(A) Phagolysosomal and cytosolic *M. tuberculosis* in a DC. Electron micrograph of a DC infected with *M. tuberculosis* for 48 hr showing different subcellular locations: (1) mycobacteria observed in membrane-enclosed phagolysosomes (asterisk) which are characterized by an electron-lucent zone between the phagosomal membrane and the bacterial cell wall and immunogold labeling with LAMP-1 on the phagolysosomal membrane. (2) Mycobacteria detected in the cytosol (encircled asterisk) lacking the enclosure of a membrane and the LAMP-1 labeling (more examples in Figures 3B, 6D, S2, and S3B). Not in this image, but detectable in low amounts, are mycobacteria in membrane-enclosed compartments lacking LAMP-1, here defined as phagosomal.

(A′) Enlargement of (A) to demonstrate that enlargement of the EM figure allows the identification of the distinguishable layers present in and around cytosolic *M. tuberculosis*. (a) cytoplasm *M. tuberculosis,* (b) plasma membrane of *M. tuberculosis* which can be discontinuous by the fixation or freezing artifacts, (c) lipid-rich cell wall also referred to as capsid, and (f) host cytosol.

(A″) Enlargement of (A) indicating additional layers present around phagosomal *M. tuberculosis.* Layers in the bacteria are identical to the cytosolic layers with the addition of two cellular layers: (d) phagosomal or electron-lucent space, which varies in size, and (e) phagosomal membrane, immunogold labeled for LAMP-1.

(B) Large clusters of cytosolic *M. tuberculosis* after 96 hr of infection. Clusters of *M. tuberculosis* present in the cytosol are abundant in nonapoptotic DCs infected for 96 hr.

(B′) Enlargement of boxed area demonstrating that phagosomal membranes do not surround these bacteria even though the lysosomal membranes are well distinguished and labeled with LAMP-1.

L indicates lysosomes, M indicates mitochondrium, asterisk indicates mycobacteria in phagolysosomes, and encircled asterisks indicate cytosolic mycobacteria. All images are from cryo-immunogold-labeled cryosections. Error bars are as follows: (A) 300 nm and (B) 500 nm.

To exclude the possibility that the appearance of cytosolic bacteria was due to reduced viability of infected DCs, we assayed the induction of apoptosis in infected DCs relative to the number of cytosolic mycobacteria. Apoptosis was analyzed using electron microscopy based on morphological features described as hallmarks for apoptosis (Kerr et al., 1972) and by immunofluorescence using Caspase 3 labeling on serial semithin sections on identical samples (van der Wel et al., 2005). Using both techniques, the percentage of apoptotic cells increased slightly between 4 and 96 hr after infection; however, a similar increase was observed in control uninfected DCs (data not shown). Furthermore, the percentage of cells containing cytosolic bacteria was three to four times greater than the percentage of apoptotic cells (Figure 4H), showing that the translocation of mycobacteria to the host cytosol occurs in nonapoptotic cells.

Translocation to the Host Cytosol Requires Mycobacterial Genes of the RD1 Region and espA

Since phagolysosomal translocation required live *M. tuberculosis* we investigated whether only virulent mycobacteria translocate to the cytosol. To address this, we compared the intracellular localization of the widely used vaccine strain *M. bovis* BCG and that of virulent *M. tuberculosis* H37Rv using both fluorescence microscopy and electron microscopy. Strikingly, BCG was restricted to membrane-enclosed compartments positive for LAMP-1 and cathepsin D at 2, 4, and 7 days of infection, and no cytosolic mycobacteria were detected in these samples

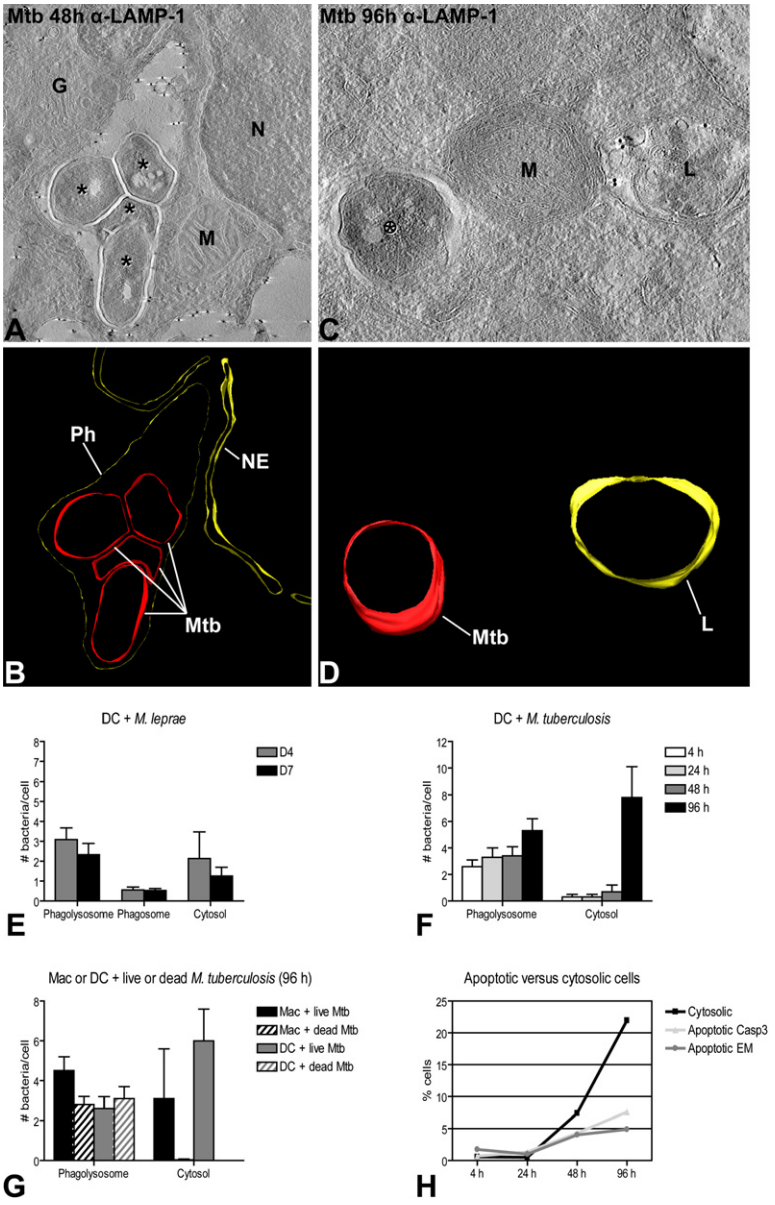

Figure 4. Tomograms of Cryosections and Number of Live *M. tuberculosis* Increases in the Cytosol

(A) Tomogram of *M. tuberculosis* in phagolysosome. A 5 nm thick tomographic slice from a 60 nm cryosection that shows a DC infected with *M. tuberculosis* for 48 hr, immunolabeled for LAMP-1 with 10 nm gold particles. The reconstruction was made from a −60° to +60° tilt series taken in 1° increments. The reconstruction was made using weighted back projection using the IMOD software (Kremer et al., 1996). Movie is available in Figure S2C.

Asterisk indicates mycobacteria in phagolysosomes, N indicates nucleus, M indicates mitochondrium, and G indicates Golgi.

(B) Model of the phagolysosomal *M. tuberculosis* tomogram. A coarse IMOD model of the tomogram in (A). The inner side of the mycobacterial (Mtb) cell wall was used to draw the model of the bacteria (red), and the total phagosomal (Ph) and nuclear envelope (NE) membrane was used to draw the model of the cellular membranes (yellow).

(C) Tomogram of *M. tuberculosis* in cytosol. A 5 nm thick tomographic slice from a 200 nm thick cryosection of DCs infected with *M. tuberculosis* for 96 hr immunolabeled for LAMP-1 with 10 nm gold particles. The reconstruction was made from a −60° to +60° tilt series taken in 1° increments. The reconstruction was made using weighted back projection using the IMOD software. The specimens were sectioned in thick (200 nm) sections to enlarge the chance of including membranous structures; however, no membranes surrounding the bacteria were detected. Movie is available in Figure S2D. Encircled asterisk indicates cytosolic *M. tuberculosis*, M indicates mitochondrium, and L indicates lysosome.

(D) Model of the cytosolic *M. tuberculosis* tomogram. IMOD model based on tomogram from (C). The inner side of the mycobacterial (Mtb) cell wall was used to draw the model of the bacteria (red), and the lysosomal (L) membrane was used to draw the model of the lysosomes (yellow).

(E) Quantification of number of *M. leprae* in different subcellular compartments. The number of *M. leprae* per infected DC as observed on immunogold EM labeled cryosections at day 4 and 7 in phagolysosomes, phagosomes, and in the cytosol. The phagolysosomal, phagosomes, and cytosolic mycobacteria are characterised as described in Figure 3A. Error bars represent standard errors. *M. leprae* resides in all compartments.

(F) Quantification of increased replication of *M. tuberculosis* in cytosol. The number of *M. tuberculosis* per infected DC at 4, 24, 48, and 96 hr after infection in different subcellular compartments as observed on immunogold EM-labeled cryosections. Data are based on at least 30 cells per time point and are a representative result out of five independent experiments. Error bars represent standard errors.

(G) Live, not dead, *M. tuberculosis* translocates in cytosol of both DCs and Macs. The number of live or heat-killed *M. tuberculosis* per macrophage and DC infected for 96 hr in phagoslysosomes and in the cytosol. Error bars represent standard error. Killed mycobacteria were only present in phagolysosomes, while live mycobacteria were translocated to the cytosol.

(H) Translocation to cytosol precedes induction of apoptosis. Percentage of cells containing cytosolic bacteria (Cytosolic) or showing apoptotic features based on the morphology in ultrathin cryosections visualized with the electron microscope (Apoptotic EM) or the presence of Caspase 3 with fluorescence microscopy (Apoptotic Casp3) at different time points after infection. After 96 hr the percentage of cells with cytosolic bacteria rapidly increases until 22%, while the percentage of apoptotic cells remains below 7%.

(Figures 5A and 5B). Although BCG failed to enter the cytosol, the number of phagolysosomal BCG and the bacterial titer increased over time (Figures 5C and 5D). This result reinforces that translocation to the cytosol does not occur simply by mycobacteria outgrowing its phagolysosomal space.

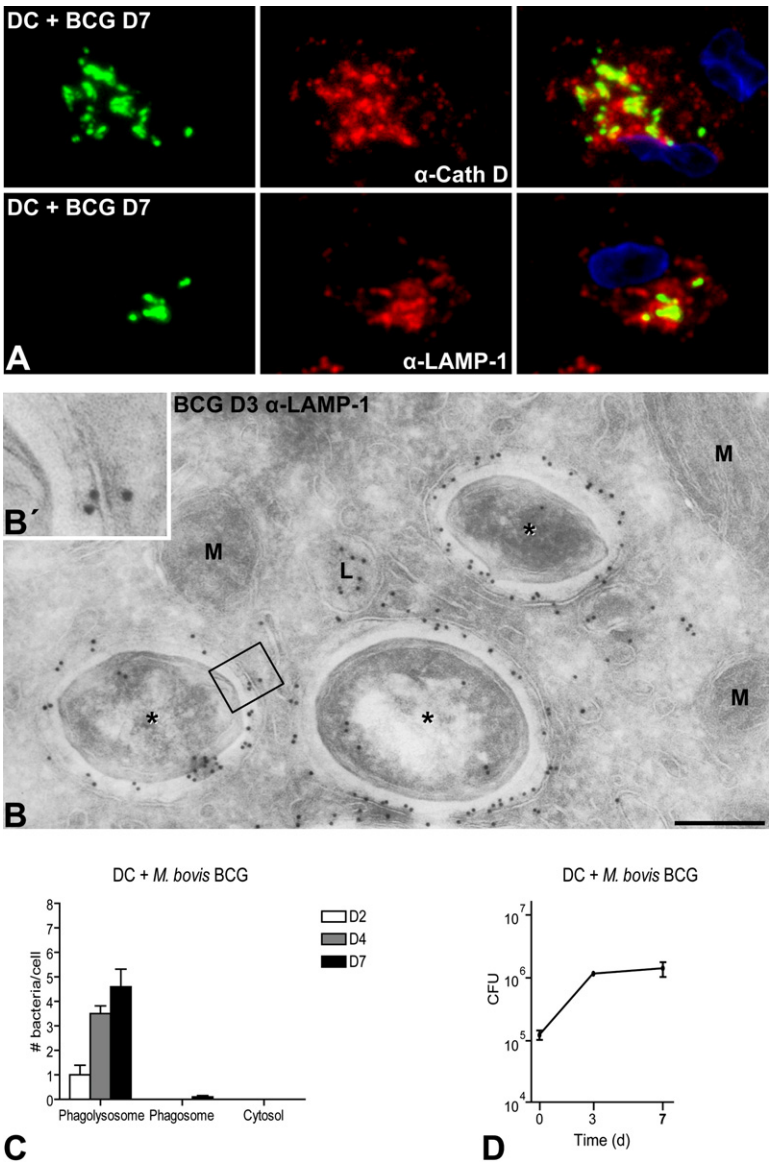

Figure 5. *M. bovis* BCG Does Not Translocate from the Phagolysosome

(A) Late in infection *M. bovis* BCG remains localized in a lysosomal compartment. DCs infected with *M. bovis* BCG (green) for 7 days show colocalization with cathepsin D or LAMP-1 (red), demonstrating that the bacteria reside in the phagolysosome (see for contrast with *M. tuberculosis* Figure 2D).

(B) *M. bovis* BCG localized in a membrane-enclosed, LAMP-1-labeled compartment. Representative EM image of DC infected with *M. bovis* BCG for 3 days and immunogold labeled for LAMP-1. *M. bovis* BCG is contained in phagolysosomes. Asterisks indicate LAMP-1-positive phagolysosomal *M. bovis* BCG. L indicates lysosomes, and M indicates mitochondrium. Bar is 200 nm.

(B′) Enlargement of boxed area demonstrating the immunogold-labeled phagosomal membrane surrounding the mycobacterial cell wall.

(C) Replication of *M. bovis* BCG in the phagolysosome. The number of *M. bovis* BCG per infected DC at 2, 4, and 7 days as observed on immunogold EM-labeled cryosections in different subcellular compartments as described in Figure 3A. Error bars represent standard error.

(D) Early replication of *M. bovis* BCG. The colony-forming units (CFU) determined for *M. bovis* BCG-infected DCs. Multiple experiments from which a representative figure is shown all demonstrated that the CFU increases over time, suggesting that replication occurs. Error bars represent standard error.

Dissection of the genetic differences between *M. tuberculosis* and BCG identified several large deletions from BCG that are present in *M. tuberculosis* and *M. leprae* (Harboe et al., 1996; Gordon et al., 1999; Behr et al., 1999; Philipp et al., 1996). From these 16 regions of difference (RD1-16) only RD1 is absent from all BCG strains thus far tested (Mostowy et al., 2002; Tekaia et al., 1999; Brosch et al., 2002). RD1 is part of a 15-gene locus known as ESX-1 that encodes a specialized secretion system dedicated to the secretion of CFP-10 and ESAT-6. In addition to the genes encoded in ESX-1, a second unlinked locus encoding *espA* is required for CFP-10 and ESAT-6 secretion (Fortune et al., 2005). The deletion of RD1 in BCG and the importance of the ESX-1 secretion system in virulence (Brodin et al., 2006) led us to test whether CFP-10 and ESAT-6 were required for *M. tuberculosis* translocation to the cytosol. This was first examined by using a *M. tuberculosis* strain containing a transposon insertion in *cfp-10* (Rv3874), which prevents the synthesis of CFP-10 and ESAT-6 (Guinn et al., 2004). Like BCG, this mutant failed to enter the host cytosol over the course of 7 days of infection and resided in LAMP-1-positive compartments (Figure 6A). Next, we used a Δ*espA* strain of *M. tuberculosis* to determine if the secretion of CFP-10 and ESAT-6 is required for the cytosolic phenotype. Following infection of DCs, the Δ*espA* strain and the Δ*espA* strain carrying the empty complementing vector (Δ*espA* pJEB; data not shown) localized to LAMP-1-positive phagolysomes, and a low percentage of mycobacteria were detected in host cytosol (Figures 6B and 6C). Strikingly, complementation of *espA* restored the number of cytosolic bacteria to a similar level as wild-type *M. tuberculosis* (Figures 6B and 6D), demonstrating a role for the ESX-1 system and the secretion of CFP-10

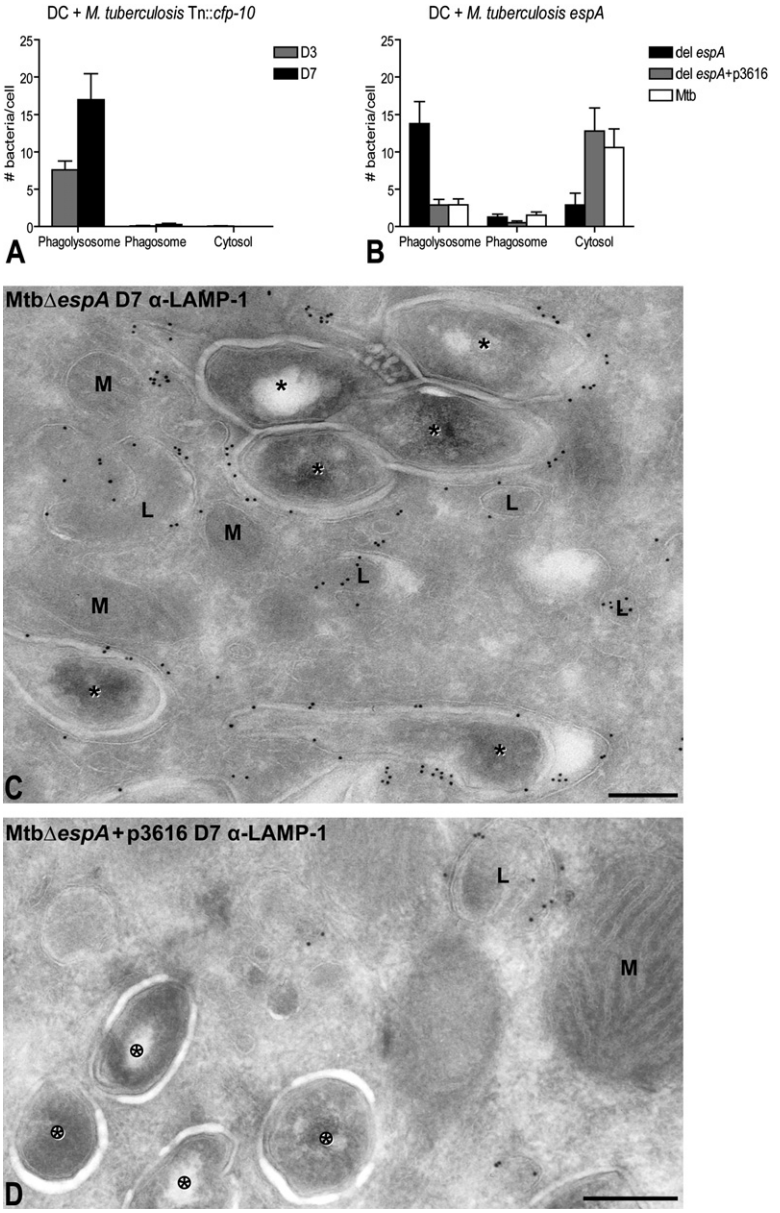

Figure 6. *M. tuberculosis* RD1 Mutants Do Not Translocate from the Phagolysosome

(A) *cfp-10* mutant of *M. tuberculosis* replicates in phagolysosome. The number of *M. tuberculosis* Tn::*cfp-10* per infected DC at 3 and 7 days as observed on immunogold EM-labeled cryosections in phagolysosomes, phagosomes, and in the cytosol as defined in legend for Figure 3A. This mutant does not translocate to the cytosol and replicates in the phagolysosomes to an average of 17 bacteria per infected cell at day 7. Error bars represent standard error.

(B) *ΔespA* mutant *M. tuberculosis* localizes in phagolysosome. The average number of *M. tuberculosis ΔespA* (delta3616), *M. tuberculosis ΔespA* reconstituted with *espA* (delta3616+p3616) and *M. tuberculosis* H37Rv per infected DC 7 days after infection. The number of bacteria was determined as described for Figure 3A. The *espA* deletion mutant does not translocate, while the complemented *espA* mutant (deta3616+p3616) and the wild-type *M. tuberculosis* H37Rv (Mtb) translocate to the cytosol.

(C) *ΔespA* mutant *M. tuberculosis* localizes in membrane-enclosed phagolysosome. Representative EM image of DC infected with *M. tuberculosis ΔespA* for 7 days and immunogold labeled for LAMP-1 demonstrates that *M. tuberculosis ΔespA* remains in a membrane-enclosed LAMP-1-labeled compartment.

(D) *ΔespA* mutant complemented with *espA* *M. tuberculosis* localizes in cytosol. Representative EM image of DC infected with *M. tuberculosis* ΔespA complemented with espA (deta3616+p3616) for 7 days showing cytosolic location; lysosomes and mitochondria show clear membranes.

Asterisks (C) indicate phagolysosomal *M. tuberculosis* ΔespA, encircled asterisks (D) indicate cytosolic *M. tuberculosis* ΔespA complemented with espA, L indicates lysosomes, and M indicates mitochondria. Bar is as follows: (C) 200 nm and (D) 300 nm.

and ESAT-6 in the translocation of *M. tuberculosis* from the host endocytic system.

To determine in an independent approach if *M. tuberculosis* replicates in the cytosol and the Tn::*cfp-10* mutant in the phagolysomes, we determined the amount of FtsZ, a bacterial tubulin-like protein. FtsZ is critical for the cell division process in many prokaryotes, including mycobacteria, and is transiently higher expressed during cytokinesis (Margolin, 2005). The relative immunogold labeling index for FtsZ was determined on mycobacteria in the cytosol and in phagolysosomal compartments at different times of infection, then compared to the labeling on cellular compartments as control (Figure S4). The data demonstrate at 7 days of infection the highest amount of FtsZ in cytosolic *M. tuberculosis* relative to phagolysosomal bacteria, suggesting that *M. tuberculosis* preferably replicates in the cytosol. In contrast, the Tn::*cfp-10* mutant replicates in the phagolysosomal compartments.

Translocation to the Host Cytosol Is Followed by Cell Death

Others have demonstrated that *M. tuberculosis* and, more specifically, ESAT-6 can induce apoptosis (Placido et al., 1997; Keane et al., 1997; Riendeau and Kornfeld, 2003; Lee et al., 2006; Derrick and Morris, 2007). We observe in DCs cultures, infected with *M. tuberculosis* for 7 days, that the amount of cell death based on Caspase 3 and EM is significantly increased. Interestingly DCs infected with mutant *M. tuberculosis* Tn::*cfp-10* showed a lower

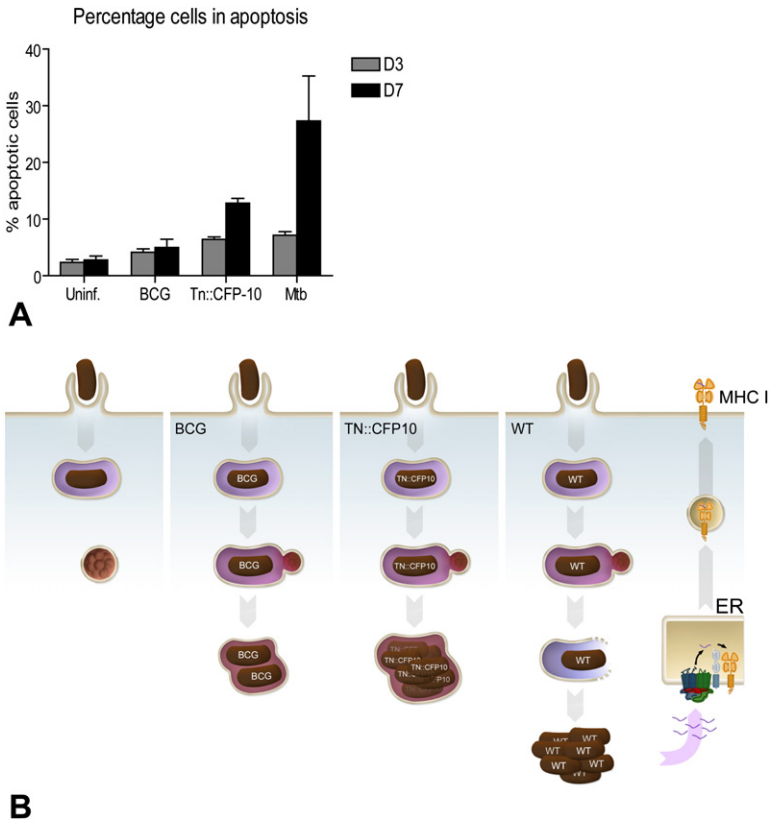

Figure 7. Cytosolic *M. tuberculosis* Induces Apoptosis and Schematic Representation Subcellular Pathway

(A) Cytosolic *M. tuberculosis* induces apoptosis. Percentage of apoptotic cells after infection with *M. tuberculosis, M. bovis* BCG, or *M. tuberculosis* Tn::*cfp-10* per infected DC and uninfected control cells at 3 and 7 days as determined with Caspase 3 labeling with fluorescence microscopy. The percentage of apoptotic cells rapidly increases after 3 days, when DCs are infected with *M. tuberculosis*, while the percentage of apoptotic cells remains below 5% for *M. bovis* BCG and uninfected control cells. *M. tuberculosis* Tn::*cfp-10*-infected cells demonstrate an intermediate percentage of apoptosis.

(B) Schematic representation of the subcellular pathway of different types of mycobacteria. The subcellular pathway of different types of mycobacteria within the host cell. Left panel represents the current view in which mycobacteria reside in an "early" phagosome. The two middle panels show traffic of *M. bovis* BCG and *M. tuberculosis* Tn::*cfp-10* after uptake, both residing and multiplying in a LAMP-1-containing membrane-enclosed compartment which fuses with lysosomes. Right panel shows virulent *M. tuberculosis* or *M. leprae* present in phagolysosomes and the subsequent translocation to the cytosol. Here possible replication, degradation, and peptide delivery to the MHC I pathway occurs.

amount of Caspase-3-positive apoptotic cells (Figure 7A). Importantly, the translocation of *M. tuberculosis* to the cytosol precedes the induction of apoptosis (see also Figure 4H).

DISCUSSION

Previous studies showed some evidence for *M. tuberculosis* that appeared to be free in the cytoplasm; however in the absence of mechanism (Myrvik et al., 1984; Leake et al., 1984; McDonough et al., 1993) using traditional "plastic-embedded" electron microscopy. It has been difficult to confirm these results, as this technique does not allow immunogold labeling and does not visualize distinctly the host phagolysosome and mycobacterial membrane bilayer (see Figure S5 and compare with, for example, Figure 1B and the electron tomographic reconstruction in Figure 4 and the moves in Figures S2C and S2D). The prevailing paradigm has remained that *M. tuberculosis* reside in the endocytic system (Orme, 2004; Vergne et al., 2004; Russell et al., 2002; Kang et al., 2005; Russell, 2001; Pizarro-Cerda and Cossart, 2006). *Mycobacterium* localization in infected macrophages has been extensively studied for over 40 years using an array of techniques and a number of *Mycobacterium* species as model organisms for *M. tuberculosis*. In general, the majority of these experimental systems only focused on the first 48 hr following infection and were often performed with avirulent mycobacteria. Here we have used an extended time course to examine the localization of *M. tuberculosis* and *M. leprae* for up to 7 days of infection. In our assays, the excellent preservation of cellular membranes in cryosections, coupled with immunological detection of endocytic markers, allowed the quantitative assessment of mycobacterial localization to the cytosol only at times beyond 2 days of infection.

In addition to *M. tuberculosis*, the RD1 locus is also present in *M. bovis, M. kansasii, M. marinum, M. africanum,* and *M. leprae* (Berthet et al., 1998; Harboe et al., 1996). The ESX-1 region has an important role in the virulence of *M. tuberculosis* (Lewis et al., 2003; Hsu et al., 2003; Stanley et al., 2003). The genes encoded in the ESX-1 region are predicted to form a specialized secretory apparatus that secretes CFP-10 and ESAT-6. Pathogens such as *L. monocytogenes* that lyse host phagosomes and replicate in the host cytosol induce potent CD8+ T cell responses (Glomski et al., 2002; Schuerch et al., 2005). Along these lines it is interesting to speculate that an analogous mechanism may function during *M. tuberculosis* infection. The intracellular expression patterns of *cfp-10*, *esat-6*, and *espA* have not been characterized in detail; however, they are clearly expressed following infection of human macrophages. Guinn et al. (2004) have reported that *M. tuberculosis* lyses host cells and spreads to uninfected macrophages over a 7 day time course and that this occurs in a RD1-dependent manner (Guinn et al.,

2004). Recently, *M. marinum* has been shown to escape with low relative numbers from phagosomes in infected macrophages and to spread to neighboring cells via actin-based motility (Stamm et al., 2003, 2005). These processes also involve CFP-10 and ESAT-6 (Gao et al., 2006). In contrast we did not find any evidence for actin tails for *M. tuberculosis*.

The immune response to *M. tuberculosis* is a dynamic process involving both CD4+ and CD8+ T cells (Flynn and Chan, 2001), which predominate as the major INFγ-secreting cells at different stages of infection: CD4+ T cells dominate during acute infection and CD8+ T cells during persistent infection (Lazarevic et al., 2005). How antigens from intracellular bacteria gain access to the MHC class I antigen-loading pathway in the ER remains an intense area of study. Several groups have suggested direct fusion between the ER and phagosome during phagocytosis (Houde et al., 2003; Ackerman et al., 2003; Guermonprez et al., 2003), however, quantitative assessment of ER markers on both model latex bead phagosomes and *M. avium*-containing phagosomes contradict those findings (Touret et al., 2005). Similarly, we find no evidence for the localization of ER markers with a cytosolic epitope to the mycobacteria containing phagosome after infection, but rather we suggest that *M. tuberculosis* and *M. leprae* antigens presented by MHC class I are most likely derived from bacteria that have entered the host cytosol as shown here (see Figure 7B). Recent in vivo work (Majlessi et al., 2005) and unpublished data presented at the 2007 TB Keystone meeting confirm this suggestion by showing a significant increase of MHC class I-restricted CD8+ T cell response in a recombinant BCG strain in which the extended RD1 region is introduced (R. Billeskov and J. Dietrich, personal communication) or by showing that the T cell response to CFP-10 and ESAT-6 is eliminated in *M. tuberculosis* mutations affecting the function of the ESX-1 secretion system (S. Behar, personal communication).

It is significant that BCG, which is used in many countries worldwide as a mycobacterial vaccine strain, remains restricted to the phagolysosome following infection of DCs and macrophages, whereas virulent *M. tuberculosis* does not (Figure 7B). BCG vaccination has questionable efficacy against the highly infectious pulmonary form of tuberculosis, and it fails to generate a strong MHC class I-restricted T cell response. The work presented here emphasizes that avirulent BCG fail to translocate the phagolysosome and suggests this may account for their poor capacity to stimulate critical CD8+ T cell responses through MHC class I (Figure 7B). Interestingly, innovative vaccine approaches have genetically engineered BCG to express LLO as a mechanism to generate more potent MHC class I-restricted responses. Indeed, LLO+ BCG are more effective vaccines than the isogenic BCG parental strain (Grode et al., 2005). Designing vaccines that mimic virulent strains in translocating into the cytosol is likely to be a critical step forward in producing more effective vaccines for tuberculosis.

EXPERIMENTAL PROCEDURES

Human Cell Cultures

Peripheral blood mononuclear cells (PBMC) were isolated from healthy human donors as previously described (Porcelli et al., 1992). CD14+ monocytes were positively selected from PBMC using CD14 microbeads and magnetic cell separation (Miltenyi Biotec, Auburn, CA). Immature human monocyte-derived DCs were prepared from CD14+ monocytes by culture in 300 U/ml of granulocyte-macrophage colony-stimulating factor (GM-CSF, Sargramostim, Immunex, Seattle, WA) and 200 U/ml of IL-4 (PeproTech, Rocky Hill, NJ) for 5 days in complete RPMI medium (10% heat-inactivated FCS/20 mM Hepes/2 mM L-glutamine/1 mM sodium pyruvate/55 μM 2-mercaptoethanol/essential and nonessential amino acids). GM-CSF and IL-4 were replenished on day 2, day 5, and day 9 after isolation. Macrophages were prepared by culture of CD14+ monocytes in IMDM with 10% human AB serum, 2 mM L-glutamine, and 50 ng/mL M-CSF (PeproTech, Rocky Hill, NJ).

Mycobacterial Infections

M. tuberculosis strains and Bacillus of Calmette and Guérin (BCG) were grown to mid-ogarithmic phase from frozen stocks in 7H9 Middlebrook media containing OADC enrichment solution and 0.05% Tween-20 for 1 week at 37°C. The wild-type *M. tuberculosis* strain used in these studies was H37Rv-expressing green fluorescent protein (GFP; Ramakrishnan et al., 2000). The BCG strain was provided by Barry Bloom. The Tn::Rv3874 (*cfp-10*) and the Δ*espA* strain (delta3616) have been previously described (Guinn et al., 2004; Fortune et al., 2005). The Δ*espA* strain complemented strain encodes *espA* under the control of its native promoter on an integrating vector (delta3616+p3616). The construct has been shown to complement the Δ*espA* mutation for ESAT-6 secretion (S. Fortune, personal communication). As a control, the delta3616 pJEB—the *espA* deletion strain with the empty vector—was used. *M. leprae* were purified from mouse footpads as previously described and were used in experiments 1 day after isolation (Adams et al., 2002).

For in vitro infections, bacteria were harvested and suspended in RPMI containing 10% FCS, 2% human serum, and 0.05% Tween 80, followed by washing in RPMI complete media. Cultures were filtered though a 5 μM syringe filter to obtain cell suspensions and were counted using a Petroff-Houser chamber. Bacteria were added to DCs and macrophage cultures at an MOI ~10, and plates were centrifuged for 2 min at 700 rpm prior to incubation at 37°C with 5% CO_2. After 1 hr, infected macrophage cultures were washed three times with warm culture media to remove free mycobacteria. For DC cultures, media was removed after 4 hr of infection, diluted ~1:6 in prewarmed RPMI complete media, centrifuged at 1000 rpm for 2 min, and resuspended in RPMI complete media supplemented with GMCSF/IL4. Culture wells were washed with RPMI three times to remove any remaining extracellular bacteria prior to replating DCs.

Colony-forming units (CFU) were enumerated by lysing infected DCs in sterile water with 0.1% saponin for 5 min. Lysed cells were repeatedly mixed, and dilutions were made in sterile saline containing Tween-20. Diluted samples were plated on 7H11 Middlebrook agar plates (Remel), and colonies were enumerated after 2 to 3 weeks of growth.

Electron Microscopy

Fixed cells were collected, embedded in gelatine, and cryosectioned with a Leica FCS and immunolabeled as described previously (Peters et al., 2006). Samples were trimmed using a diamond Cryotrim 90 knife at −100°C (Diatome, Switzerland), and ultrathin sections of 50 nm were cut at −120°C using a Cryoimmuno knife (Diatome, Switzerland). More details on immunolabeling are in the Supplemental Data.

Supplemental Data

Supplemental Data include Experimental Procedures, five figures, and References and can be found with this article online at http://www.cell.com/cgi/content/full/129/7/1287/DC1/.

ACKNOWLEDGMENTS

We would like to acknowledge Jacques Neefjes, Tom Ottenhof, Chris Mercogliano, Wilbert Bitter, Ben Appelmelk, Mark Marsh, the Bram Koster laboratory, and all members of the Peters laboratory for their critical comments and useful suggestions. We are grateful to Barry Bloom for supplying the BCG Pasteur strain, Jim Krahenbuhl for supplying purified *M. leprae*, Malini Rajagopalan for the FtsZ antibody, and Sarah Fortune and Eric Rubin for making the *cfp-10* and *espA* mutant strains available. We thank Alex Griekspoor for graphical work and Nico Ong for the photography work. The Netherlands Leprosy Relief (NLS) gave seven years of financial support. D.L.H. is a Damon Runyan Fellow supported by the Damon Runyon Cancer Research Foundation (DRG-1814-04).

Received: May 2, 2006
Revised: October 18, 2006
Accepted: May 9, 2007
Published: June 28, 2007

REFERENCES

Ackerman, A.L., Kyritsis, C., Tampe, R., and Cresswell, P. (2003). Early phagosomes in dendritic cells form a cellular compartment sufficient for cross presentation of exogenous antigens. Proc. Natl. Acad. Sci. USA *100*, 12889–12894.

Adams, L.B., Scollard, D.M., Ray, N.A., Cooper, A.M., Frank, A.A., Orme, I.M., and Krahenbuhl, J.L. (2002). The study of Mycobacterium leprae infection in interferon-gamma gene–disrupted mice as a model to explore the immunopathologic spectrum of leprosy. J. Infect. Dis. *185* (*Suppl 1*), S1–S8.

Armstrong, J.A., and Hart, P.D. (1971). Response of cultured macrophages to Mycobacterium tuberculosis, with observations on fusion of lysosomes with phagosomes. J. Exp. Med. *134*, 713–740.

Behr, M.A., Wilson, M.A., Gill, W.P., Salamon, H., Schoolnik, G.K., Rane, S., and Small, P.M. (1999). Comparative genomics of BCG vaccines by whole-genome DNA microarray. Science *284*, 1520–1523.

Berthet, F.X., Rasmussen, P.B., Rosenkrands, I., Andersen, P., and Gicquel, B. (1998). A Mycobacterium tuberculosis operon encoding ESAT-6 and a novel low-molecular-mass culture filtrate protein (CFP-10). Microbiol. *144*, 3195–3203.

Brodin, P., Majlessi, L., Marsollier, L., de Jonge, M.I., Bottai, D., Demangel, C., Hinds, J., Neyrolles, O., Butcher, P.D., Leclerc, C., et al. (2006). Dissection of ESAT-6 system 1 of Mycobacterium tuberculosis and impact on immunogenicity and virulence. Infect. Immun. *74*, 88–98.

Brosch, R., Gordon, S.V., Marmiesse, M., Brodin, P., Buchrieser, C., Eiglmeier, K., Garnier, T., Gutierrez, C., Hewinson, G., Kremer, K., et al. (2002). A new evolutionary scenario for the Mycobacterium tuberculosis complex. Proc. Natl. Acad. Sci. USA *99*, 3684–3689.

Derrick, S.C., and Morris, S.L. (2007). The ESAT6 protein of Mycobacterium tuberculosis induces apoptosis of macrophages by activating caspase expression. Cell Microbiol *9*, 1547–1555.

Flynn, J.L., and Chan, J. (2001). Immunology of tuberculosis. Annu. Rev. Immunol. *19*, 93–129.

Fortune, S.M., Jaeger, A., Sarracino, D.A., Chase, M.R., Sassetti, C.M., Sherman, D.R., Bloom, B.R., and Rubin, E.J. (2005). Mutually dependent secretion of proteins required for mycobacterial virulence. Proc. Natl. Acad. Sci. USA *102*, 10676–10681.

Gao, L.Y., Pak, M., Kish, R., Kajihara, K., and Brown, E.J. (2006). A mycobacterial operon essential for virulence in vivo and invasion and intracellular persistence in macrophages. Infect. Immun. *74*, 1757–1767.

Glomski, I.J., Gedde, M.M., Tsang, A.W., Swanson, J.A., and Portnoy, D.A. (2002). The Listeria monocytogenes hemolysin has an acidic pH optimum to compartmentalize activity and prevent damage to infected host cells. J. Cell Biol. *156*, 1029–1038.

Gordon, S.V., Brosch, R., Billault, A., Garnier, T., Eiglmeier, K., and Cole, S.T. (1999). Identification of variable regions in the genomes of tubercle bacilli using bacterial artificial chromosome arrays. Mol. Microbiol. *32*, 643–655.

Grode, L., Seiler, P., Baumann, S., Hess, J., Brinkmann, V., Nasser Eddine, A., Mann, P., Goosmann, C., Bandermann, S., Smith, D., et al. (2005). Increased vaccine efficacy against tuberculosis of recombinant Mycobacterium bovis bacille Calmette-Guerin mutants that secrete listeriolysin. J. Clin. Invest. *115*, 2472–2479.

Guermonprez, P., Saveanu, L., Kleijmeer, M., Davoust, J., Van Endert, P., and Amigorena, S. (2003). ER-phagosome fusion defines an MHC class I cross-presentation compartment in dendritic cells. Nature *425*, 397–402.

Guinn, K.M., Hickey, M.J., Mathur, S.K., Zakel, K.L., Grotzke, J.E., Lewinsohn, D.M., Smith, S., and Sherman, D.R. (2004). Individual RD1-region genes are required for export of ESAT-6/CFP-10 and for virulence of Mycobacterium tuberculosis. Mol. Microbiol. *51*, 359–370.

Harboe, M., Oettinger, T., Wiker, H.G., Rosenkrands, I., and Andersen, P. (1996). Evidence for occurrence of the ESAT-6 protein in Mycobacterium tuberculosis and virulent Mycobacterium bovis and for its absence in Mycobacterium bovis BCG. Infect. Immun. *64*, 16–22.

Houde, M., Bertholet, S., Gagnon, E., Brunet, S., Goyette, G., Laplante, A., Princiotta, M.F., Thibault, P., Sacks, D., and Desjardins, M. (2003). Phagosomes are competent organelles for antigen cross-presentation. Nature *425*, 402–406.

Hsu, T., Hingley-Wilson, S.M., Chen, B., Chen, M., Dai, A.Z., Morin, P.M., Marks, C.B., Padiyar, J., Goulding, C., Gingery, M., et al. (2003). The primary mechanism of attenuation of bacillus Calmette-Guerin is a loss of secreted lytic function required for invasion of lung interstitial tissue. Proc. Natl. Acad. Sci. USA *100*, 12420–12425.

Kang, P.B., Azad, A.K., Torrelles, J.B., Kaufman, T.M., Beharka, A., Tibesar, E., DesJardin, L.E., and Schlesinger, L.S. (2005). The human macrophage mannose receptor directs Mycobacterium tuberculosis lipoarabinomannan-mediated phagosome biogenesis. J. Exp. Med. *202*, 987–999.

Keane, J., Balcewicz-Sablinska, M.K., Remold, H.G., Chupp, G.L., Meek, B.B., Fenton, M.J., and Kornfeld, H. (1997). Infection by Mycobacterium tuberculosis promotes human alveolar macrophage apoptosis. Infect. Immun. *65*, 298–304.

Kerr, J.F., Wyllie, A.H., and Currie, A.R. (1972). Apoptosis: a basic biological phenomenon with wide-ranging implications in tissue kinetics. Br. J. Cancer *26*, 239–257.

Kremer, J.R., Mastronarde, D.N., and McIntosh, J.R. (1996). Computer visualization of three-dimensional image data using IMOD. J. Struct. Biol. *116*, 71–76.

Lazarevic, V., Nolt, D., and Flynn, J.L. (2005). Long-term control of Mycobacterium tuberculosis infection is mediated by dynamic immune responses. J. Immunol. *175*, 1107–1117.

Leake, E.S., Myrvik, Q.N., and Wright, M.J. (1984). Phagosomal membranes of Mycobacterium bovis BCG-immune alveolar macrophages are resistant to disruption by Mycobacterium tuberculosis H37Rv. Infect. Immun. *45*, 443–446.

Lee, J., Remold, H.G., Ieong, M.H., and Kornfeld, H. (2006). Macrophage apoptosis in response to high intracellular burden of Mycobacterium tuberculosis is mediated by a novel caspase-independent pathway. J. Immunol. *176*, 4267–4274.

Lewis, K.N., Liao, R., Guinn, K.M., Hickey, M.J., Smith, S., Behr, M.A., and Sherman, D.R. (2003). Deletion of RD1 from Mycobacterium tuberculosis mimics bacille Calmette-Guerin attenuation. J. Infect. Dis. *187*, 117–123.

Majlessi, L., Brodin, P., Brosch, R., Rojas, M.J., Khun, H., Huerre, M., Cole, S.T., and Leclerc, C. (2005). Influence of ESAT-6 secretion system 1 (RD1) of Mycobacterium tuberculosis on the interaction between mycobacteria and the host immune system. J. Immunol. *174*, 3570–3579.

Margolin, W. (2005). FtsZ and the division of prokaryotic cells and organelles. Nat. Rev. Mol. Cell Biol. *6*, 862–871.

McDonough, K.A., Kress, Y., and Bloom, B.R. (1993). Pathogenesis of tuberculosis: interaction of Mycobacterium tuberculosis with macrophages. Infect. Immun. *61*, 2763–2773.

Mostowy, S., Cousins, D., Brinkman, J., Aranaz, A., and Behr, M.A. (2002). Genomic deletions suggest a phylogeny for the Mycobacterium tuberculosis complex. J. Infect. Dis. *186*, 74–80.

Myrvik, Q.N., Leake, E.S., and Wright, M.J. (1984). Disruption of phagosomal membranes of normal alveolar macrophages by the H37Rv strain of Mycobacterium tuberculosis. A correlate of virulence. Am. Rev. Respir. Dis. *129*, 322–328.

Orme, I. (2004). Adaptive immunity to mycobacteria. Curr. Opin. Microbiol. *7*, 58–61.

Peters, P.J., Neefjes, J.J., Oorschot, V., Ploegh, H.L., and Geuze, H.J. (1991). Segregation of MHC class II molecules from MHC class I molecules in the Golgi complex for transport to lysosomal compartments. Nature *349*, 669–676.

Peters, P.J., Bos, E., and Griekspoor, A. (2006). Cryo-immunogold electron microscopy. In Current Protocols Cell Biology (Hoboken, NJ: John Wiley & Sons), pp. 4.7.1–4.7.19.

Philipp, W.J., Nair, S., Guglielmi, G., Lagranderie, M., Gicquel, B., and Cole, S.T. (1996). Physical mapping of Mycobacterium bovis BCG pasteur reveals differences from the genome map of Mycobacterium tuberculosis H37Rv and from M. bovis. Microbiol. *142*, 3135–3145.

Pizarro-Cerda, J., and Cossart, P. (2006). Bacterial adhesion and entry into host cells. Cell *124*, 715–727.

Placido, R., Mancino, G., Amendola, A., Mariani, F., Vendetti, S., Piacentini, M., Sanduzzi, A., Bocchino, M.L., Zembala, M., and Colizzi, V. (1997). Apoptosis of human monocytes/macrophages in Mycobacterium tuberculosis infection. J. Pathol. *181*, 31–38.

Porcelli, S., Morita, C.T., and Brenner, M.B. (1992). CD1b restricts the response of human CD4–8- T lymphocytes to a microbial antigen. Nature *360*, 593–597.

Ramakrishnan, L., Federspiel, N.A., and Falkow, S. (2000). Granuloma-specific expression of Mycobacterium virulence proteins from the glycine-rich PE-PGRS family. Science *288*, 1436–1439.

Riendeau, C.J., and Kornfeld, H. (2003). THP-1 cell apoptosis in response to Mycobacterial infection. Infect. Immun. *71*, 254–259.

Russell, D.G. (2001). Mycobacterium tuberculosis: here today, and here tomorrow. Nat. Rev. Mol. Cell Biol. *2*, 569–577.

Russell, D.G., Mwandumba, H.C., and Rhoades, E.E. (2002). Mycobacterium and the coat of many lipids. J. Cell Biol. *158*, 421–426.

Schuerch, D.W., Wilson-Kubalek, E.M., and Tweten, R.K. (2005). Molecular basis of listeriolysin O pH dependence. Proc. Natl. Acad. Sci. USA *102*, 12537–12542.

Stamm, L.M., Morisaki, J.H., Gao, L.Y., Jeng, R.L., McDonald, K.L., Roth, R., Takeshita, S., Heuser, J., Welch, M.D., and Brown, E.J. (2003). Mycobacterium marinum escapes from phagosomes and is propelled by actin-based motility. J. Exp. Med. *198*, 1361–1368.

Stamm, L.M., Pak, M.A., Morisaki, J.H., Snapper, S.B., Rottner, K., Lommel, S., and Brown, E.J. (2005). Role of the WASP family proteins for Mycobacterium marinum actin tail formation. Proc. Natl. Acad. Sci. USA *102*, 14837–14842.

Stanley, S.A., Raghavan, S., Hwang, W.W., and Cox, J.S. (2003). Acute infection and macrophage subversion by Mycobacterium tuberculosis require a specialized secretion system. Proc. Natl. Acad. Sci. USA *100*, 13001–13006.

Stevens, J.M., Galyov, E.E., and Stevens, M.P. (2006). Actin-dependent movement of bacterial pathogens. Nat. Rev. Microbiol. *4*, 91–101.

Tekaia, F., Gordon, S.V., Garnier, T., Brosch, R., Barrell, B.G., and Cole, S.T. (1999). Analysis of the proteome of Mycobacterium tuberculosis in silico. Tuber. Lung Dis. *79*, 329–342.

Touret, N., Paroutis, P., Terebiznik, M., Harrison, R.E., Trombetta, S., Pypaert, M., Chow, A., Jiang, A., Shaw, J., Yip, C., et al. (2005). Quantitative and dynamic assessment of the contribution of the ER to phagosome formation. Cell *123*, 157–170.

van der Wel, N.N., Sugita, M., Fluitsma, D.M., Cao, X., Schreibelt, G., Brenner, M.B., and Peters, P.J. (2003). CD1 and major histocompatibility complex II molecules follow a different course during dendritic cell maturation. Mol. Biol. Cell *14*, 3378–3388.

van der Wel, N.N., Fluitsma, D.M., Dascher, C.C., Brenner, M.B., and Peters, P.J. (2005). Subcellular localization of mycobacteria in tissues and detection of lipid antigens in organelles using cryo-techniques for light and electron microscopy. Curr. Opin. Microbiol. *8*, 323–330.

Vergne, I., Chua, J., Singh, S.B., and Deretic, V. (2004). Cell biology of mycobacterium tuberculosis phagosome. Annu. Rev. Cell Dev. Biol. *20*, 367–394.